MOLECULAR AND CELLULAR BIOLOGY, Nov. 2000, p. 8560–8570 Vol. 20, No. 22
0270-7306/00/$04.00+0

DNA Replication Progresses on the Periphery of Nuclear Aggregates Formed by the BCL6 Transcription Factor

OLIVIER ALBAGLI,[1]* CATHERINE LINDON,[1] DANIÈLE LANTOINE,[2] SABINE QUIEF,[2] EDMOND PUVION,[3] CHRISTIAN PINSET,[1] AND FRANCINE PUVION-DUTILLEUL[3]

CNRS URA 1947, Institut Pasteur, 75015 Paris,[1] INSERM U524, IRCL, 59045 Lille,[2] and CNRS UPR 1983, 94801 Villejuif,[3] France

Received 30 May 2000/Returned for modification 6 July 2000/Accepted 21 August 2000

The *BCL6* proto-oncogene, frequently alterated in non-Hodgkin lymphoma, encodes a POZ/zinc finger protein that localizes into discrete nuclear subdomains. Upon prolonged BCL6 overexpression in cells bearing an inducible *BCL6* allele (UTA-L cells), these subdomains apparently coincide with sites of DNA synthesis. Here, we explore the relationship between BCL6 and replication by both electron and confocal laser scanning microscopy. First, by electron microscope analyses, we found that endogenous BCL6 is associated with replication foci. Moreover, we show that a relatively low expression level of BCL6 reached after a brief induction in UTA-L cells is sufficient to observe its targeting to mid, late, and at least certain early replication foci visualized by a pulse-labeling with bromodeoxyuridine (BrdU). In addition, when UTA-L cells are simultaneously induced for BCL6 expression and exposed to BrdU for a few hours just after the release from a block in mitosis, a nuclear diffuse BCL6 staining indicates cells in G_1, while cells in S show a more punctate nuclear BCL6 distribution associated with replication foci. Finally, ultrastructural analyses in UTA-L cells exposed to BrdU for various times reveal that replication progresses just around, but not within, BCL6 subdomains. Thus, nascent DNA is localized near, but not colocalized with, BCL6 subdomains, suggesting that they play an architectural role influencing positioning and/or assembly of replication foci. Together with its previously function as transcription repressor recruiting a histone deacetylase complex, BCL6 may therefore contribute to link nuclear organization, replication, and chromatin-mediated regulation.

The *BCL6* proto-oncogene (also known as *LAZ3*) has been cloned because of its frequent structural alteration, and presumably misregulation, in non-Hodgkin lymphomas (33, 55). BCL6 harbors both a conserved and self-interacting BTB/POZ domain at its N terminus and six Krüppel-like zinc fingers involved in specific DNA binding at its C terminus (1, 17, 33, 55). Like some other, but not all, BTB/POZ and zinc finger proteins, BCL6 appears to act as a transcriptional repressor recruiting a SMRT/SIN3A/histone deacetylase (HDAC) repression complex, suggesting that it influences transcription in part by locally modifying the histone acetylation status and hence the chromatin structure of its target genes (14, 18, 23, 29). BCL6 is a regulator of lymphoid development and function (11, 15, 54), though it may also play an important role in other cell types, possibly by controlling the balance between apoptosis and terminal differentiation (2, 3, 39).

A distinctive feature of the nuclear BTB/POZ proteins is that they often concentrate into nuclear subdomains (8, 11, 13, 17, 29). For instance, in *Drosophila*, endogenous Mod (Mdg4)/E(var)3-93D localizes to dots near the nuclear periphery, while in the early embryo, the GAGA factor, which, like BCL6, also contains a zinc finger DNA-binding region, displays a punctate distribution associated with centromeric heterochromatin (22, 45). Moreover, at least in some cases, the formation of these nuclear subdomains undergoes cell cycle control, as, in larval tissues, the GAGA factor moves every cell cycle between a heterochromatic (punctate) localization in M phase to a euchromatic (diffuse) localization in interphase (44). In most cases, however, the identity and function of the nuclear subdomains defined or revealed by the BTB/POZ proteins are unknown. Elucidating the nature and function(s) of these subdomains is likely to shed light onto the role of nuclear BTB/POZ proteins, as well as provide important information regarding the mechanisms underlying the compartmentalization of nuclear functions.

One such regionalized nuclear function is DNA replication. DNA replication occurs at discrete nuclear subdomains termed replication foci, each comprising a few synchronously fired replicons, the proteins necessary for replication, and the nascent DNA, which can be revealed by an in vivo incorporation of halogenated deoxyuridines such as bromodeoxyuridine (BrdU) (30, 40, 42). The genome is replicated in a sequential fashion during S phase, and the number, position, and shape of the replication foci are characteristic of an S-phase substep and highly reproduced throughout successive S phases. Each of these substeps corresponds to the replication of different chromatin domains, with the transcribed euchromatin being replicated first and the usually silent heterochromatin replicated at the end (40, 42; see below). Moreover, the clustering and nuclear positioning of the DNA sequences replicated at individual replication foci are precisely maintained through the cell cycle and into subsequent generations, so that the BrdU foci persist as discrete structures even when replication does not occur (19, 30, 40, 48, 51). How this highly precise and reliable nuclear regionalization is achieved is still poorly understood, although the nuclear matrix is generally believed to be implicated (12, 26, 40, 41, 50, 51).

Both endogenous and overexpressed BCL6 localizes into discrete nuclear subdomains (3, 11, 17, 29), hereafter referred to as nuclear aggregates. Using UTA-L cells, which express an epitope-tagged version of BCL6 upon removal of tetracycline from the culture medium, we previously reported that the large BCL6 aggregates formed upon BCL6 overexpression coincide

* Corresponding author. Present address: CNRS UPR 1983, BP 8, 7 rue Guy Môquet, 94801 Villejuif, France. Phone: (33)1 49 58 33 70. Fax: (33)1 49 58 33 81. E-mail: oalbagli@vjf.cnrs.fr.

in some cell nuclei with the DNA replication foci identified by a 90-min pulse-labeling with BrdU (3). We made this observation in unsynchronized UTA-L cells upon prolonged BCL6 induction (48 h), under which conditions BCL6 impairs progression throughout S phase and triggers apoptosis (3). Using electron and laser scanning confocal microscopy, we explore here the relationship between replication foci and both overexpressed and endogenous BCL6. Electron microscope analyses in a lymphoid cell line reveal that endogenous BCL6 can also associate with replication foci. In UTA-L cells, we show that BCL6 is differentially distributed in G_1 and S nuclei and appears associated with replication foci during early, mid, and late S. Moreover, BCL6 aggregates of UTA-L cell nuclei are progressively wrapped by newly replicated DNA, leading to a close apposition but not true colocalization of the two stainings. Altogether, these findings support the idea that BCL6 aggregates may play an architectural role in replication, by influencing replication foci assembly and/or positioning.

MATERIALS AND METHODS

Antibodies. Monoclonal primary antibodies used were anti-BrdU (Boehringer GmbH, Mannheim, Germany) and anti-Flag M2 (Sigma-Aldrich, Lisle D'Abeau Chesnes, France). Polyclonal primary antibodies used were rabbit anti-BCL6 C19 and N3 (Santa Cruz Biotechnology, Santa Cruz, Calif.). Secondary antibodies were either fluorescein isothiocyanate-coupled donkey anti-mouse antibody (Jackson ImmunoResearch, West Grove, Pa.) and Cy3-coupled donkey anti-rabbit antibody (Jackson) (Fig. 2 and 4) or Alexa 488-coupled goat anti-rabbit antibody and Alexa 594-coupled goat anti-mouse antibody (Molecular Probes, Eugene, Oreg.) (Fig. 5). For ultrastructural studies, secondary antibodies were gold-labeled goat anti-mouse immunoglobulin G (IgG) antibody and goat anti-rabbit IgG (British Biocell International Ltd., Cardiff, United Kingdom). All primary and secondary antibodies used in immunofluorescence experiments were diluted 1/100 or 1/200 in phosphate-buffered saline (PBS)–0.2% gelatin (2). For ultrastructural studies, primary and secondary antibodies were diluted 1/10 and 1/25, respectively, in PBS.

Cell culture and synchronization. UTA-L cells (3) were cultured at 37°C and 5% CO_2 in a 50/50 mixture of MCDB 202 (Bicef, L'Aigle, France) and Dulbecco modified Eagle medium supplemented with 10% fetal calf serum (Biomedia, Boussens, France) (growth medium [GM]) plus tetracycline (2 μg/ml; Sigma-Aldrich), hygromycin (200 μg/ml; Boehringer), and G418 (500 μg/ml; Gibco BRL, Cergy-Pontoise, France) (GM/tet will hereafter denote GM plus tetracycline [2 μg/ml]). Karpas 422 cells were grown in RPMI medium supplemented with 10% fetal calf serum (Gibco-BRL).

For long BCL6 induction, UTA-L cells were rinsed twice with GM, then trypsinized and collected by centrifugation, and rinsed twice more before plating to efficiently remove tetracycline. Under these conditions, at least half of the cells were induced after 20 to 40 h.

UTA-L cells in M phase of the cell cycle were obtained by a double thymidine-nocodazole block essentially as described elsewhere (38). Briefly, UTA-L cells were plated at 30 to 40% confluency in GM/tet supplemented with 2 mM thymidine (Sigma-Aldrich). After 30 h, cells were rinsed two times with GM, cultured in GM/tet alone for about 15 h, and then treated again with 2 mM thymidine. After 24 h, thymidine was removed again; 6 h later, cells were treated with nocodazole (200 ng/ml; Sigma-Aldrich) for a further 16 h. Cells in M phase of the cell cycle were collected by rinsing the dishes, then centrifuged and washed twice to remove both tetracyline and nocodazole, and then plated in GM plus BrdU (using a Boehringer BrdU labeling and detection kit). After 6 h, 10 to 20% of the cells displayed detectable expression of BCL6 expression as measured by immunofluorescence experiments (intermediate induction), while 50 to 70% were stained with the anti-BrdU monoclonal antibody upon immunofluorescence, in agreement with data obtained by fluorescence-activated cell sorting (FACS) analyses upon propidium iodide staining. To prevent entry into S phase, L-mimosine (0.5 mM; Sigma-Aldrich) (37) was added together with BrdU just after release from the nocodazole block.

Finally, brief BCL6 induction was obtained by rinsing exponentially growing, asynchronous UTA-L cells four times and then exposing them to GM for 4 h. Under these conditions, only a few UTA-L cells (2 to 5%) were positive for BCL6 expression as measured by immunofluorescence experiments.

FACS analyses. For FACS analyses, the collected cells were fixed in ice-cold 70% ethanol and incubated in a propidium iodide (10 μM)-RNase (50 μg/ml) solution for 1 h at room temperature for DNA staining and analyzed by FACS (Becton Dickinson) as previously described (3).

Immunofluorescence. In all immunofluorescence experiments shown, the anti-BCL6 polyclonal antibody C19 was used. Double BCL6-BrdU staining was performed as previously described (3). In brief, cells were fixed in formalin (Sigma-Aldrich) for 10 min at room temperature, treated for 10 min in a PBS–0.25% Triton solution at room temperature, and incubated sequentially with the rabbit anti-BCL6 antibody C19 and the anti-rabbit secondary antibody. The cells were then fixed again in formalin (10 min at room temperature), treated with 1 N HCl for 20 min at room temperature, and stained for BrdU using a BrdU labeling and detection kit as instructed by the manufacturer. All observations were made using a Leica laser scanning confocal microscope and Kodak Ektachrome 400 film.

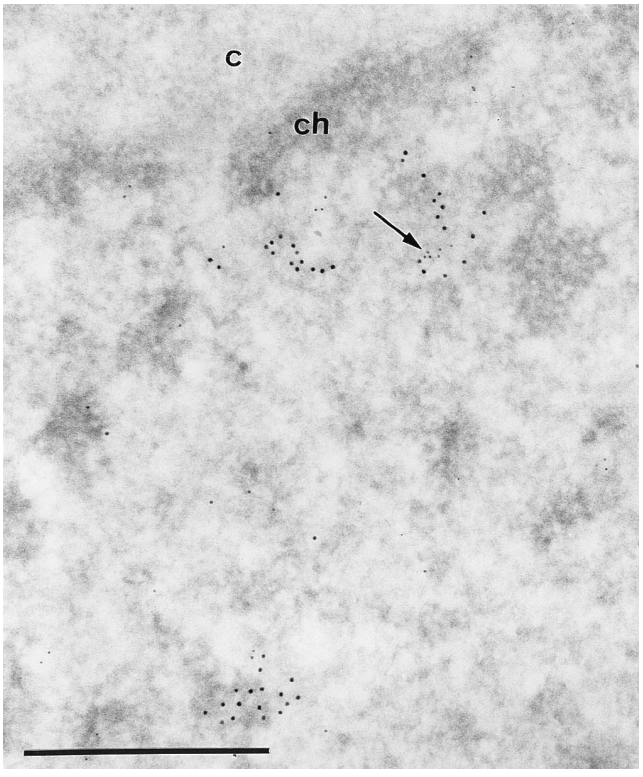

FIG. 1. Endogenous BCL6 is associated with replication foci in lymphoid Karpas 422 cells. Images show simultaneous visualization at the ultrastructural level of BCL6 and BrdU-containing DNA following a 15-min pulse. The arrow points to a cluster of BCL6 (polyclonal antibody N3 and 5-nm gold particles) located among the BrdU-containing DNA molecules (monoclonal anti-BrdU antibodies and 10-nm gold particles). c, cytoplasm; ch, perinuclear condensed chromatin. Bar, 0.5 μm.

Electron microscopy. Cells were fixed with 4% formaldehyde (Merck, Darmstadt, Germany) in 0.1 M Sörensen phosphate buffer (pH 7.3 to 7.4) for 1 h at 4°C prior to methanol dehydration and Lowicryl K4M (Polysciences Europe Gmbh, Eppelheim, Germany) embedding. Polymerization was carried out under long-wavelength UV light (Philips TL 6W fluorescent tubes) at −30°C. Ultrathin (80 nm thick) sections were collected on Formvar-carbon-coated gold grids (200 mesh). Grids bearing Lowicryl sections were floated for 1 h on 5-μl drops of primary antibody prior to incubation for 30 min over 5-μl drops of secondary antibodies conjugated to gold particles, 10 nm in diameter, and finally stained with 5% aqueous uranyl acetate for 10 min.

Localization of newly replicated DNA was examined following incorporation of BrdU by the living cells for different periods of time. At the end of the pulse treatments, cells were fixed with formaldehyde and embedded in Lowicryl K4M. To render the BrdU incorporated into the DNA strands accessible to the antibodies, grids bearing Lowicryl sections were floated on a 10-μl drop of 5 N HCl for 25 min as previously described (9). Subsequently, BrdU was immunodetected as follows. Grids were transferred successively for a few minutes over 10-μl drops of PBS and 5% bovine serum albumin (BSA) in PBS and for 1 h over 5-μl drops of anti-BrdU antibody diluted in PBS with 1% BSA and 2 μl of Triton X-100 per ml. After rapid washes over drops of PBS, grids were incubated for 30 min on 5-μl drops of goat anti-mouse IgG conjugated to gold particles, either 5 or 10 nm in diameter diluted in PBS with BSA and Triton X-100. After washing and air drying, grids were observed following 10 min of staining with uranyl acetate. For the simultaneous detection of BCL6 and BrdU, grids with HCl pretreatment were incubated over a mixture of primary antibodies for 1 h and then over a mixture of secondary antibodies conjugated to different sizes of gold particles (5 and 10 nm in diameter) for 30 min.

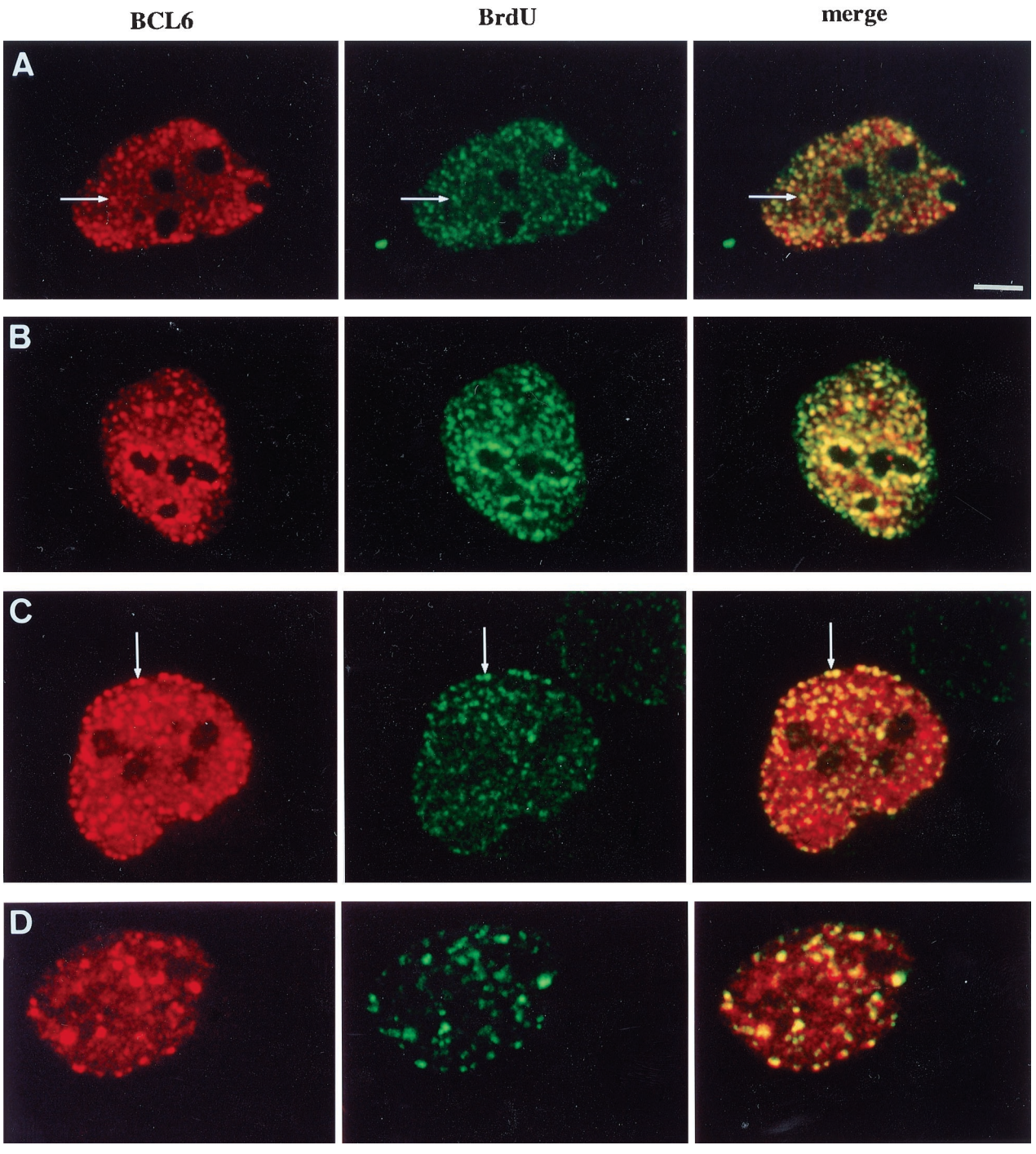

FIG. 2. BCL6 is associated with replication foci throughout most of S phase. Vertebrate cells undergoing replication show a typical sequence of replication foci patterns. Unsynchronized UTA-L cells were induced for BCL6 expression during 4 h, then pulse-labeled (15 min) with BrdU, and submitted to laser scanning confocal microscopy to detect both BCL6 (red) and BrdU (green) by immunofluorescence. The pattern of replication was assigned to early (A), mid (B and C), and late (D) S phase according to reference 42 (see text). BCL6 appears to be associated with replication foci throughout most of S phase, as its staining concentrates in certain early replication foci (A, arrow), and decorates some mid (B and C, arrow) and late (D) replication foci. Bar, 5 μm.

RESULTS

Endogenous BCL6 is associated with replication foci. To validate our attempt to explore the relationship between BCL6 and replication foci, we first examined whether they are also associated in cells that do not artificially overexpress BCL6. Endogenous BCL6 is generally expressed at very low levels and is virtually undetectable by immunofluorescence in UTA-L cells. Thus, we used electron microscope analyses which were sensitive enough to localize endogenous BCL6. The lymphoid Karpas cell line, which expresses endogenous BCL6 at levels detectable by immunoprecipitation (17), was chosen for this study. Cells were pulse-labeled with BrdU and then costained

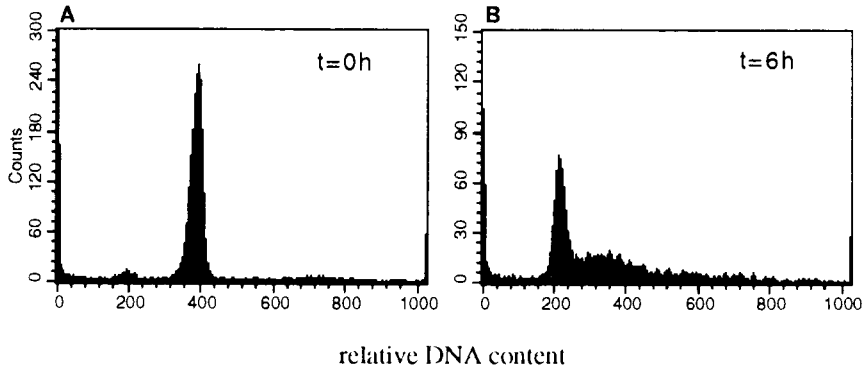

FIG. 3. Synchronization of UTA-L cells. UTA-L cells were synchronized in mitosis by a double thymidine block followed by overnight exposure to nocodazole (see Materials and Methods). Poorly attached cells were then collected and stained for relative DNA content with propidium iodide. FACS analyses demonstrated that the vast majority (>95%) of them were in mitosis (A). They were next simultaneously released from the nocodazole block and plated in BrdU-supplemented, tetracycline-free medium to induce BCL6. After 6 h, 50 to 70% of the cells had entered S phase, while almost all of the remaining cells were in G_1, as indicated by FACS analyses upon propidium iodide staining (B).

with both anti-BrdU and anti-BCL6 antibodies. Immunogold labeling shows that some BCL6 signal can be found close to the BrdU staining (Fig. 1). The 10-nm gold particles which localized BrdU accumulate over large areas (up to 300 nm in diameter). Quantitative evaluations of the electron microscope micrographs reveal that 30% of the BrdU clumps contain smaller areas (up to 30 nm in diameter) labeled with the 5-nm gold particles. This frequency of association of the two kinds of label is underevaluated because of the small size of the BCL6 areas which, therefore, are probably frequently located outside the plane of the section. We conclude that at least a fraction of endogenous BCL6 is present in the vicinity of replication foci.

BCL6 targeting toward replication foci upon mild overexpression in UTA-L cells. Having shown the association of endogenous BCL6 with replication foci, we pursued our analyses in UTA-L cells, which offer the most suitable system to localize BCL6 upon confocal and electron microscopy. However, to parallel what we observed in Karpas cells, we next studied the distribution of BCL6 with respect to replication foci, revealed by a 15-min BrdU pulse, in UTA-L cells upon a brief (4-h) induction, which gives rise to much lower BCL6 levels than the 48 h of induction that we previously used (3). Again, under these conditions, we observed a striking coincidence or overlapping between the BCL6 staining and the replication foci in some cells (Fig. 2). Confirming the mild BCL6 overexpression even at the individual cell level, the replication foci appear unaffected with respect to size, number, and shape in briefly induced compared to noninduced UTA-L (Fig. 2 and data not shown), while a long induction alters the distribution of replication foci in a manner suggesting that BCL6 can bundle or reorganize them (see below). Thus, the localization of both endogenous BCL6 (in Karpas cells) and briefly induced exogenous BCL6 (in UTA-L cells) indicates that the targeting of BCL6 toward replication foci in UTA-L cells does not rely on its vast overexpression.

BCL6 appears associated with replication foci throughout most of S phase. Replication foci undergo typical morphological changes corresponding to the replication of different chromatin domains during their progression throughout S phase. In early-S-phase cells, the replication foci appear as numerous small foci scattered throughout the nuclear interior and mainly involved in replication of the transcribed, hyperacetylated histone H4-rich chromatin (48). Later, more discrete perinucleolar and perinuclear foci (mid-S) followed by few and larger intranuclear foci (late S) replicate the heterochromatin (42). As a brief BCL6 induction has no apparent effect on replication focus morphology, we took advantage of these changes to examine whether the association between BCL6 and replication foci is specific to some substeps of the S phase. As shown in Fig. 2B and C, BCL6 is concentrated in clusters of perinucleolar as well as perinuclear mid-S replication foci. Moreover, at least a subset of the late-S large intranuclear replication foci are associated with large BCL6 nuclear dots (Fig. 2D). Thus, BCL6 is associated with replication foci from mid to late S, while the increasing size of BCL6 nuclear aggregates markedly parallels that of replication foci. Note that the colocalization is often partial and displays a great heterogeneity in relative intensity even within a single nucleus. The association of BCL6 with early replication foci is more difficult to address, given that they are small and numerous, resulting in a nearly diffuse micropunctate BrdU staining. We note, however, that the nuclei displaying a typical early-S BrdU staining also show a micropunctate BCL6 staining. Moreover, some areas of stronger BrdU staining coincide with areas of stronger BCL6 staining (Fig. 2A), indicating that at least a subset of early replication foci are decorated by the anti-BCL6 antibody. We conclude that BCL6 appears to be associated with replication foci throughout most of S phase.

BCL6 subnuclear localization in G_1 and S cells. We next examined whether BCL6 is differentially distributed within UTA-L cells in the G_1 phase of the cell cycle versus cells in S phase by restricting the start of BCL6 accumulation to late M or, more likely, G_1 and early S. To this end, UTA-L cells were synchronized in mitosis (Fig. 3A) and, when released from the block, simultaneously induced for BCL6 expression and exposed to BrdU. After 6 h, 50 to 70% of the UTA-L cells have entered the S phase as revealed by their relative DNA content upon cytofluorometric analyses (Fig. 3B), while 10 to 20% express detectable, though variable, levels of BCL6 as indicated by immunofluorescence experiments (see below). Upon this intermediate BCL6 induction and continuous exposure to BrdU, the BCL6 staining either is primarily nuclear diffuse or appears as nuclear aggregates superimposed on a diffuse background of variable intensity.

We thus observe the following correlations. (i) The vast majority of cells displaying a diffuse BCL6 staining are negative for BrdU (Fig. 4, top row). As cytofluorometric analyses indicated that very few cells are still in M at this time (Fig. 3), we conclude that most of these BCL6 nuclear diffuse, BrdU-negative cells are in G_1. (ii) The vast majority of the cells positive for both BCL6 and BrdU display some coincidence of the two stainings, suggesting that a fraction of BCL6 is concentrated to

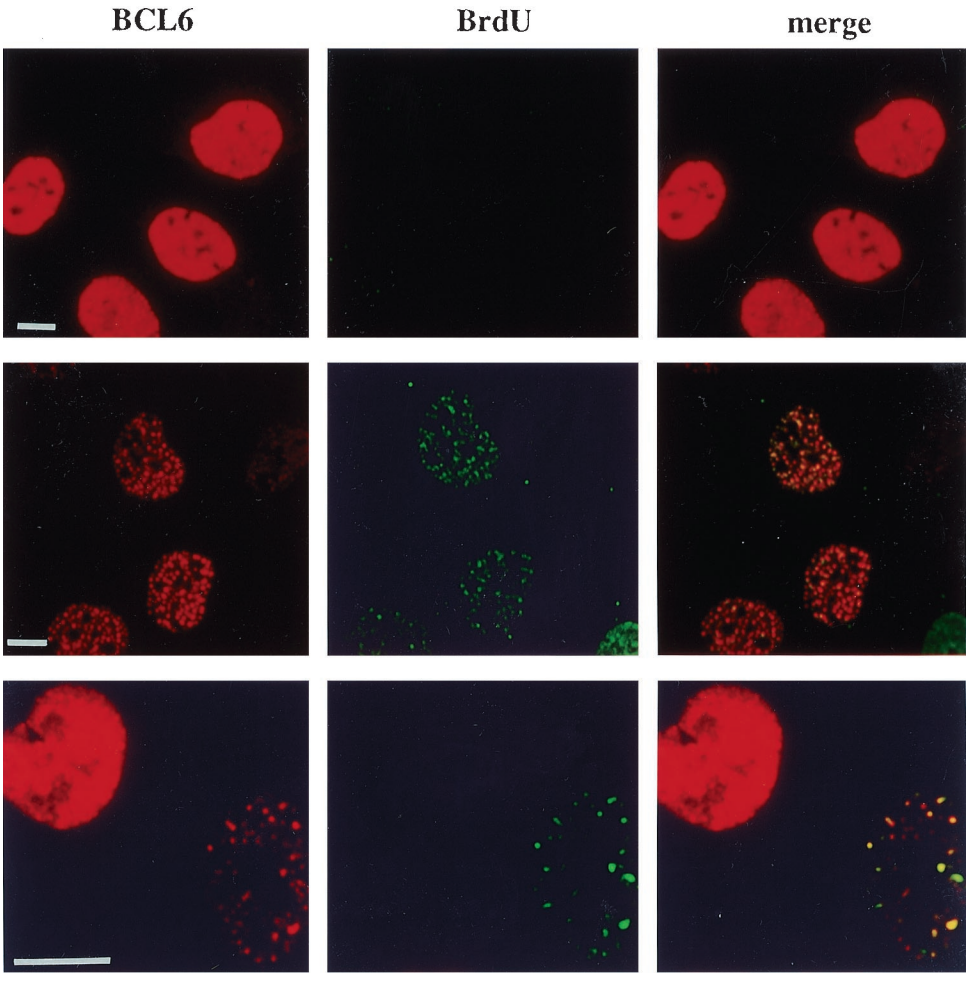

FIG. 4. BCL6 localization in G_1- and S-phase cells. UTA-L cells were synchronized in mitosis, then simultaneously induced for BCL6, and exposed to BrdU as described for Fig. 3. After 6 h, they were submitted to immunofluorescence to detect both BCL6 (red) and BrdU (green) by laser scanning confocal microscopy. We observed that (i) cells displaying a diffuse BCL6 nuclear staining are almost systematically negative for BrdU (top row) and therefore very likely in G_1 (see Fig. 3) and (ii) cells positive for both BCL6 and BrdU almost systematically display a punctate BCL6 nuclear distribution showing some coincidence with the BrdU staining (middle row). The two patterns are shown in neighboring cells, indicating that the BCL6 punctate staining does not solely result from higher expression levels. Indeed, the diffuse (presumably in an G_1-phase cell [left]), BCL6 staining can be stronger than the punctated, replication-associated distribution observed in an S-phase cell (right) (bottom row). Note that a given nucleus shows some nuclear dots containing both BrdU and BCL6 together, as well as BrdU foci with little or no BCL6 staining and vice versa. Bars, 10 μm.

replication foci when its synthesis begins between M and early S (Fig. 4, middle row).

Interestingly, BCL6 also associates with replication foci in nuclei containing a very faint, if any, underlying diffuse nuclear BCL6 staining (Fig. 4, middle and bottom rows). Moreover, the diffuse BCL6 staining in cells negative for BrdU can be much stronger than the punctate staining associated with replication foci in BrdU-positive cells (Fig. 4, bottom row). This shows that the expression level is not the sole determinant of the subnuclear partitioning of BCL6 that we observe in S-phase cells under these conditions. Altogether, these results suggest that BCL6 is nuclear diffuse in G_1 and present at least in certain replication foci during S.

To corroborate this conclusion, UTA-L cells were synchronized, induced for BCL6 expression, exposed to BrdU as described above, and compared with respect to BCL6 distribution between cells progressing into S phase and cells blocked in late G_1, using L-mimosine (37). We found that among BCL6-positive nuclei, BCL6 staining is much more often diffuse in L-mimosine-blocked cells than in untreated cells (88% diffuse plus 12% punctate and 43.5% diffuse plus 56.6% punctate, respectively, [means of two independent experiments] [Fig. 5]). This is consistent with the idea that under these conditions, BCL6 is predominantly diffuse in G_1 and forms nuclear aggregates associated with replication foci in S. Note, however, that a few cells negative for BrdU in both untreated and L-mimosine-treated cells exhibit regularly shaped spherical BCL6 nuclear aggregates often superimposed on a strong diffuse nuclear background (not shown). Thus, the assembly of BCL6 nuclear aggregates is not entirely dependent on the entry into S phase but is also determined by other, yet unknown cell cycle-related events and/or by the expression level achieved in our inducible system. We nevertheless conclude that cell cycle, and especially progression into S, might influence BCL6 subnuclear localization in UTA-L cells.

BCL6 immunolocalization in UTA-L cells at an ultrastructural level. For ultrastructural analyses, UTA-L cells were induced for 20 h (long induction, allowing most of the cells to express detectable level of BCL6) and then subjected to electron microscope analyses using either polyclonal or monoclo-

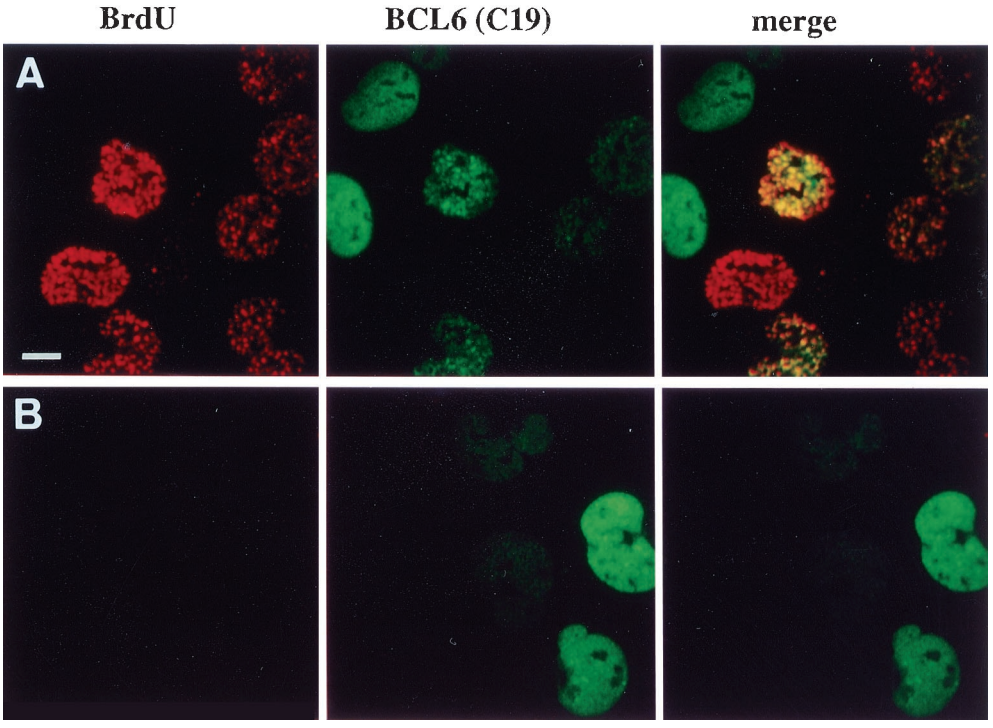

FIG. 5. Blocking cell cycle progression alters the subnuclear distribution of BCL6. UTA-L cells were synchronized in mitosis and then both induced for BCL6 and exposed to BrdU for 6 h as described for Fig. 3 in the absence (A) or presence (B) of 0.5 mM L-mimosine, which blocks the cells in late G_1 (37). Untreated cells expressing BCL6 typically show either nuclear diffuse or nuclear punctate BCL6 staining (green), corresponding to BrdU-negative (presumably in G_1) or BrdU-positive (in S; detected in red) cells, as shown in Fig. 4, top or middle row, respectively (A). In contrast, L-mimosine-treated cells are almost completely devoid of BrdU staining, as expected, and most show nuclear diffuse BCL6 staining (B). Bar, 10 μm.

nal antibodies to detect BCL6. All of the antibodies gave indistinguishable results, with BCL6 staining appearing in either of two major shapes, which are generally mutually exclusive in a given cell. Up to 50% contained a new structure (which was absent in noninduced UTA-L cells) identifiable by its electron opacity alone upon routine staining with uranyl acetate and mainly, but not exclusively, present in the nucleus (Fig. 6). It varies from 250 nm to 1.6 μm in diameter and displays a very regular aspect of either full spheres uniformly labeled with the antibody or empty spheres labeled only over the electron-opaque ring, the electron-translucent core being always devoid of gold particles (Fig. 6A). We hereafter refer to these large BCL6 aggregates as BCL6 macroaggregates. In the nucleus, these BCL6 macroaggregates are located in the interchromatin space sometimes close to the nucleolus (Fig. 6B) and do not show preferential association with other nuclear substructures such as the clusters of interchromatin granules and coiled bodies.

In about half of the remaining cells, the labeling consists of smaller (<250 nm) and more irregularly shaped clusters of gold particles which are present over the nucleus or the cytoplasm (Fig. 6C). The clusters of gold particles are superimposed on small moderately electron-opaque structures. We refer to these smaller BCL6 aggregates as BCL6 microaggregates. Like the macroaggregates, the BCL6 nuclear microaggregates are present mainly in the interchromatin space but occasionally also in association with the border or the interior of the nucleolus. It is likely that the BCL6 macroaggregates arise as a result of strong BCL6 expression, as they are scarcer upon shorter induction (data not shown), although we do not know whether they are overaggregated derivatives of BCL6 microaggregates or distinct structures.

In addition, each cell shows a slight diffuse labeling consisting of a few gold particles randomly scattered over the interchromatin space (except the enclosed clusters of interchromatin granules and coiled bodies) in the nucleus and over the ribosome-rich areas in the cytoplasm, indicating the existence of a pool of nonaggregated BCL6 molecules in both the nucleus and the cytoplasm. Finally, in contrast to the BCL6 relative RP58, which associates predominantly with condensed chromatin (6), neither the BCL6 aggregates nor the nonaggregated BCL6 pool exhibits a marked preference for a heterochromatic localization.

Nascent DNA progressively wraps around BCL6 nuclear aggregates. To examine the distribution of BCL6 nuclear aggregates with respect to newly replicated DNA, we used electron microscope analyses and BrdU pulses of various lengths. When strongly induced UTA-L cells were briefly pulse-labeled with BrdU (5 min), a faint staining of BrdU was found near some BCL6 nuclear macroaggregates (Fig. 7A). Moreover, when the induced UTA-L cells were exposed to longer pulses of BrdU (either 15 or 90 min), BrdU staining was seen not to become superimposed on the BCL6 macroaggregates but rather to progress around them (Fig. 7B to D). Thus, electron microscope analyses reveal that the apparent colocalization of BrdU staining and BCL6 nuclear aggregates by immunofluorescence is in fact a close and relatively sustained appositioning of the two labelings.

To confirm this, we performed double labeling with anti-BCL6 and anti-BrdU antibodies. This reveals that some weak BCL6 staining was sometimes present just outside the BCL6 macroaggregates which was only occasionally embedded within the BrdU staining (Fig. 8A). Most evidently, however, the vast majority of the BrdU clumps adjacent to BCL6 macro-

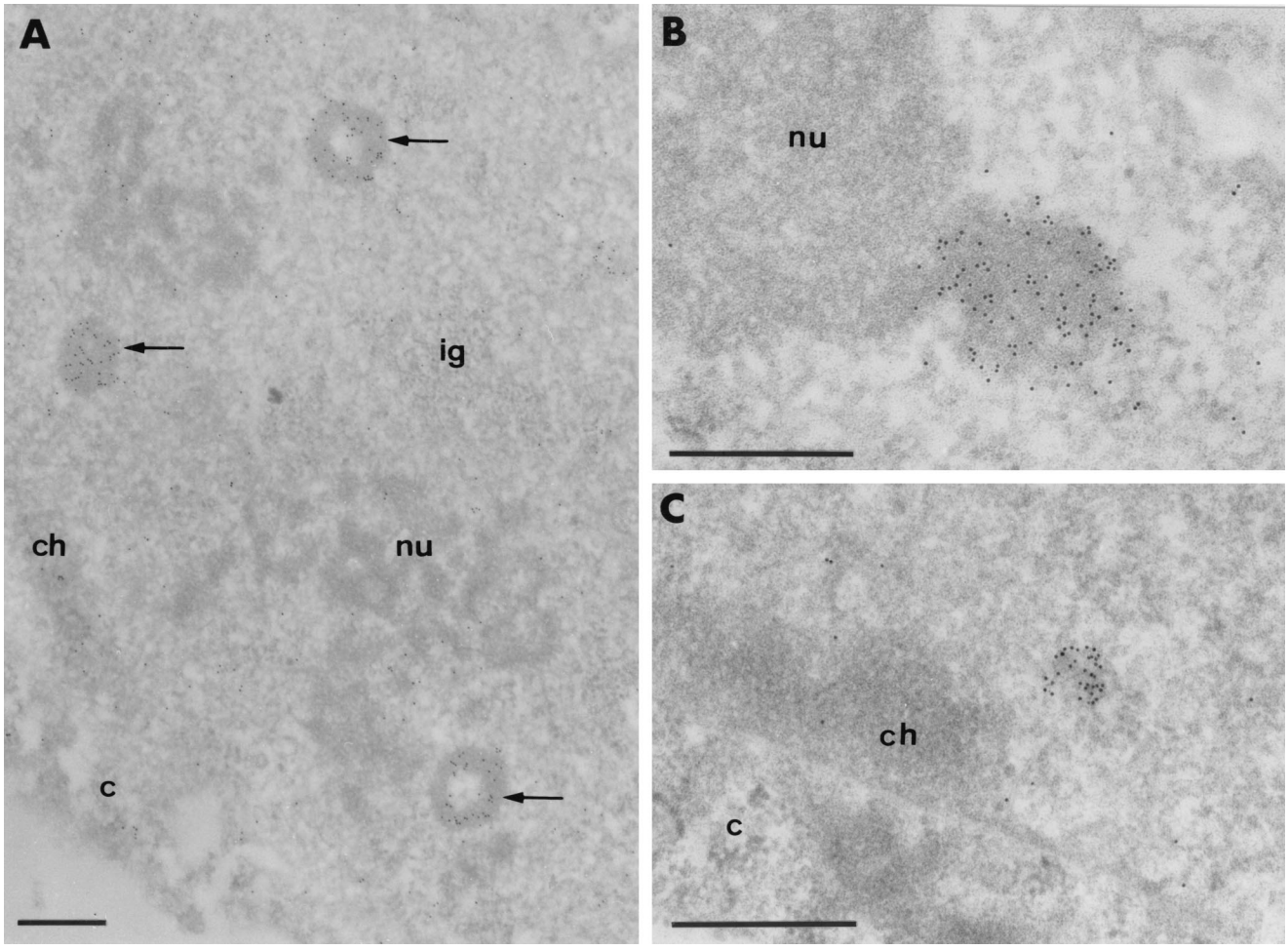

FIG. 6. Intranuclear BCL6-containing aggregates are not preferentially associated with condensed chromatin. Images show ultrastructural localization of BCL6 in UTA-L cells induced for 20 h using monoclonal antibody M2. Gold particles which localize BCL6 accumulate over newly formed, electron-dense structures in the nucleoplasm. (A) Three labeled structures (BCL6 macroaggregates; arrows). Two structures exhibit a ring-shaped configuration. (B) BCL6 macroaggregate juxtaposed to the nucleolus. (C) Smaller aggregate (BCL6 microaggregate) located at the border of the nucleus but not in contact with the perinuclear layer of condensed chromatin. Identical results were obtained with either the N3 or C19 polyclonal anti-BCL6 antibody (data not shown). c, cytoplasm; ch, perinuclear condensed chromatin; ig, cluster of interchromatin granules; nu, nucleolus. Bars, 0.5 μm.

aggregates showed no BCL6 staining, suggesting that the two labelings were indeed in close apposition rather than truly colocalized (Fig. 8B). Similar results were obtained for BCL6 microaggregates (Fig. 8C). We conclude that in UTA-L cells, replication can occur in the vicinity of, and progresses around, the BCL6 nuclear aggregates.

DISCUSSION

In this study, we explored the relationship between BCL6 transcription factor and sites of ongoing DNA synthesis. We show that a fraction of both endogenous (in Karpas cells) and mildly overexpressed (in UTA-L cells) BCL6 is present in replication foci. Furthermore, in UTA-L cells, a few-hour of induction of BCL6 concomitant with continuous exposure to BrdU just after synchronization in mitosis is sufficient to reveal the targeting of BCL6 toward subnuclear regions coinciding with replication foci. Under the same conditions, a nuclear diffuse BCL6 distribution almost invariably indicates G_1 cells. Thus, one aspect of the BCL6 subnuclear partitioning appears as a cell cycle-regulated event.

The association between putative transcription factors and replication foci is not without precedent. Of interest is IKAROS, which shows parallels with BCL6. IKAROS is another self-interacting zinc finger DNA-binding transcriptional regulator that also recruits HDAC-containing complexes and regulates lymphoid differentiation (24, 35, 36). Moreover, IKAROS undergoes a cell cycle-dependent subnuclear redistribution, giving first a diffuse staining mainly excluding the heterochromatin in resting lymphocytes, which partially concentrates to numerous speckles, and then into few large foci (toroids) as the cells progress throughout G_1. Finally, IKAROS associates with replication foci and negatively regulates the entry into S (7, 24, 35, 36). However, the large G_1 IKAROS foci are close to centromeric heterochromatin and, consistently, IKAROS associates only with late replication foci whereas BCL6 staining also appears to decorate some early (presumably euchromatic) replication foci and, accordingly, does not show a preferential localization in heterochromatin at least upon overexpression.

What could be the role(s) of BCL6 in replication foci? BCL6 coprecipitates with an HDAC activity and binds HDAC1 in vitro (15, 19). Replication is likely to represent a window of time permitting certain covalent modifications of DNA or hi-

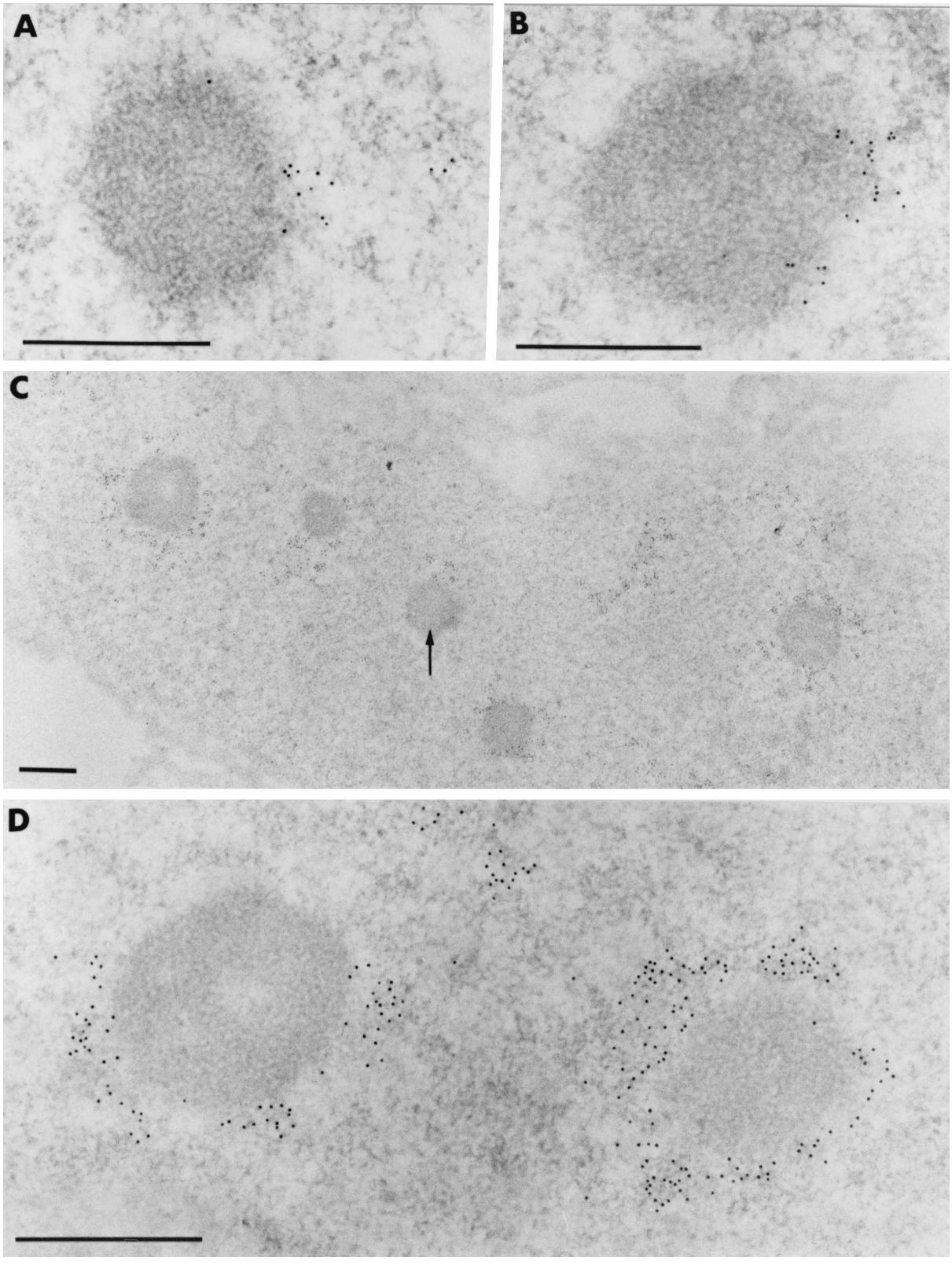

FIG. 7. Newly synthesized DNA progressively wraps around the intranuclear BCL6-containing aggregates. Images show ultrastructural distribution of BrdU-containing DNA in UTA-L cells induced for 20 h. Following short (5-min [A] and 15-min [B]) pulse-labelings, gold particles which localize BrdU are restricted to limited portions of the fibrillar clear halo which surrounds the BCL6 macroaggregates. No labeling occurs over the macroaggregates themselves. Following a 90-min pulse, (C and D), a crown of gold particles entirely surrounds certain BCL6 macroaggregates, while others are only partially surrounded (arrow in panel C). In all cases, however, the BCL6 aggregates themselves are entirely devoid of BrdU labeling, as shown at low magnification in panel C. Bars, 0.5 μm.

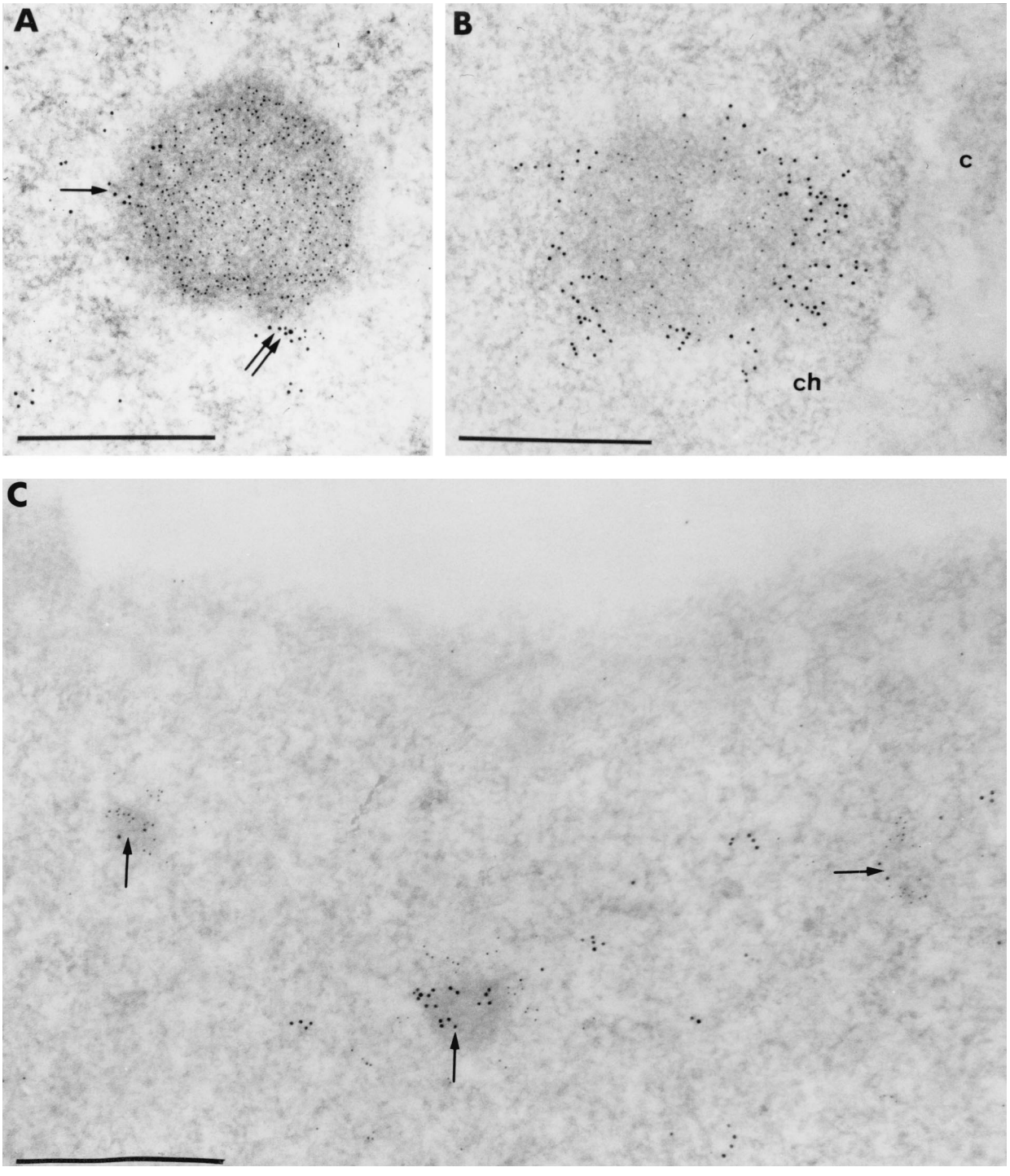

FIG. 8. Newly synthesized DNA and BCL6 are located in two juxtaposed, concentric domains. Images show simultaneous visualization at the ultrastructural level of BCL6 (polyclonal antibodies: N3 [A and B] and C19 [C]) and BrdU-containing DNA (monoclonal anti-BrdU antibody) in UTA-L cells induced for 20 h. (A and B) Gold particles, 5 nm in diameter, label the BCL6 protein, whereas the 10-nm gold particles label the BrdU. (A) Following a short (5-min) pulse, a small cluster of 10-nm gold particles only (arrow) and a cluster of mixed 5- and 10-nm gold particles (double arrow) are close to a BCL6 macroaggregate decorated only by 5-nm gold particles. (B) Following a 90-min pulse, the BCL6 macroaggregate is stained only with anti-BCL6 antibodies (5-nm gold particles), whereas it is surrounded by a crown of 10-nm gold particles only. c, cytoplasm; ch, perinuclear condensed chromatin. (C) In this nucleus, BCL6 constitutes microaggregates (arrows) labeled with the 10-nm gold particles. Following a 15-min pulse, the clumps of BrdU (5-nm gold particles) are closely juxtaposed to the BCL6 microaggregates. Bars, 0.5 μm.

stones to ensure the assembly of chromatin and the establishment or maintenance of chromatin domains underlying epigenetic stable transcriptional regulation (5, 7, 35, 49). One of these modifications is the deacetylation of histones just after their deposition onto newly synthesized DNA. Class I HDACs (HDAC1 to -3) have been suggested to contribute to this step of chromatin maturation (21, 47), and indeed, HDAC1 is somewhat concentrated in certain BCL6- or BrdU-costained

foci (O. Albagli, C. Lemercier, S. Khochbin, and F. Puvion-Dutilleul, unpublished data). Class II HDACs (HDAC4- to -7), which interact with SMRT/NcoR (28, 31) and colocalize with BCL6 upon overexpression (Albagli et al., unpublished data), may also be recruited into replication foci. Moreover, chromatin remodeling complexes are believed to modulate the accessibility of DNA not only for transcription but also for replication (4). For instance, the carboxy terminus of BRCA1 both associates with HDAC1/2 and stimulates the activity of a yeast replication origin when artificially tethered near it (27, 53). Thus, BCL6-recruited HDACs may in turn participate in replication initiation, chromatin maturation, and/or BCL6-mediated transcriptional regulation. That BCL6 appears present in replication foci throughout most of S phase is more consistent with a role in origin recognition or remodeling or in chromatin maturation rather than a restricted effect on the chromatin environment of specific target genes. The role of BCL6 may thus differ from that envisioned for IKAROS, whereby IKAROS tethers the NURD-HDAC complex to heterochromatic regions and contributes to heterochromatin-specific modifications, although the nuclear diffuse IKAROS fraction may recruit other chromatin-remodeling complexes to euchromatin (35, 36).

At an ultrastructural level, BCL6 aggregates are compact structures (almost devoid of surrounding BCL6 staining), while replication progresses around them, resulting in a close apposition but not colocalization of the two labelings. After a 90-min BrdU incorporation, a pulse length exceeding the lifetime of a given replication focus (19, 40), this apposition persists to give large BrdU rings whose shape and size appear to be imposed by the BCL6 aggregates, as they are not observed in uninduced UTA-L cells. Given that replication and transcription sites appear in close proximity (but distinct) (52), it is possible that this apposition reflects that the true localization of BCL6 is the transcription sites which overgrow upon BCL6 overexpression, thereby becoming wrapped by the neighboring nascent DNA. However, this apposition can be observed irrespective of the size of the BCL6 nuclear aggregates and even upon very short pulses of BrdU. Thus, perhaps underlying its ability to disturb S-phase progression (3), this persistent apposition could rather indicate that BCL6 overexpression remodels nuclear organization and replication foci positioning, possibly by mediating their coalescence and/or by altering the local concentration of replication proteins. Several lines of evidence indeed indicate that BTB/POZ proteins contribute to nuclear organization. They often self-aggregate and heteroaggregate through their BTB/POZ domain-containing N termini, leaving available, in most cases, numerous bundled DNA-binding or Kelch (putative actin-binding) domains at the C termini (1, 8, 46). Accordingly, much as the cytoskeletal BTB/POZ Kelch protein cross-links actin fibers (46), they mediate long-range interactions between distant DNA sequences (1, 56), a property that may contribute to their role in the activity of certain insulators (20, 22, 43). In the case of the GAGA factor, this leads a promoter containing multiple GAGA-binding sites to wrap around GAGA aggregates in vitro (32) in a manner reminiscent of the organization of newly replicated DNA around BCL6 nuclear aggregates in vivo. Moreover, another BTB/POZ protein forms dots in the nuclear periphery and may repress transcription by housing DNA sequences, possibly in association with DNA-binding proteins, into this nuclear environment (13). Finally, BCL6 aggregates are resistant to detergent and nuclease extraction (Albagli et al., unpublished data), suggesting that like several BTB/POZ proteins (22, 34), they are bound to nuclear matrix, an underlying structure believed to organize higher-order chromatin domains and anchor replication apparatus (13, 44, 55, 56). Interestingly, the positioning of chromatin domains within the nucleus might determine when they are replicated during S (19, 40, 48). Moreover, there is also a correlation between replication timing and chromatin structure or transcriptional activity, which may explain why some regulators of S-phase progression modify position effect variegation in *Drosophila* (19, 27, 48). Although this nuclear compartmentalization usually appears highly stable and clonally inherited, it may sometimes undergo developmentally regulated modifications. For instance, IKAROS is believed to recruit its target genes toward the centromeric heterochromatin, to which IKAROS foci are also closely apposed, an effect that correlates both with their heritable silencing and a change in their replication timing (10). These findings reveal an interplay between chromatin structure, replication timing, and nuclear organization (16) and suggest that transcription factors forming discrete aggregates associated with both chromatin-remodeling complexes and replication foci are likely actors in this interplay. We thus propose that BCL6 is also involved in this interplay in the following manner. In G_1, BCL6 could contribute to the positioning of many chromatin domains, thereby leading to its diffuse localization. As the cells enter S phase, BCL6 might further aggregate in discrete foci, possibly as a result of posttranslational modifications. This event may in turn locally alter the concentration of replication proteins as well as HDAC-containing complexes, hence influencing both the organization and activity of the replication foci and the chromatin structure of the newly synthesized DNA. Thus, BCL6 might contribute to link DNA positioning, replication timing, and chromatin-mediated transcriptional regulation.

ACKNOWLEDGMENTS

Raymond Hellio and Pascal Roux are warmly thanked for the confocal microscope analyses. We are also indebted to Claire Vourc'h for helpful advice, Evelyne Pichard for technical assistance, Sylvie Besse-Souquere for the figures, and Jean-Pierre Kerckaert for support.

This work is supported by grants from INSERM, CNRS, Association pour la Recherche contre le Cancer (ARC), Ligue Nationale contre le Cancer, Association Française contre les Myopathies (AFM), and Fondation de France.

REFERENCES

1. **Albagli, O., P. Dhordain, C. Deweindt, G. Lecocq, and D. Leprince.** 1996. The BTB/POZ domain: a new protein/protein interaction motif common to DNA- and actin-binding proteins. Cell Growth Differ. **6:**1495–1503.
2. **Albagli, O., P. Dhordain, D. Lantoine, F. Auradé, S. Quief, J. P. Kerckaert, D. Montarras, and C. Pinset.** 1998. Increased expression of the LAZ3 (BCL6) proto-oncogene accompanies murine skeletal myogenesis. Differentiation **64:**33–44.
3. **Albagli, O., D. Lantoine, S. Quief, F. Quignon, C. Englert, J. P. Kerckaert, D. Montarras, C. Pinset, and C. Lindon.** 1999. Overexpressed BCL6 (LAZ3) oncoprotein triggers apoptosis, delays S phase progression and associates with replication foci. Oncogene **18:**5063–5075.
4. **Alexiadis, V., P. D. Varga-Weisz, E. Bonte, P. Becker, and C. Gruss.** 1998. In vitro chromatin remodelling by chromatin accessibility complex (CHRAC) at the SV40 origin of replication. EMBO J. **17:**3428–3438.
5. **Almouzni, G., and A. P. Wolffe.** 1993. Replication-coupled chromatin assembly is required for the repression of basal transcription in vivo. Genes Dev. **7:**2033–2047.
6. **Aoki, K., G. Meng, K. Suzuki, T. Takashi, Y. Kameoka, K. Nakahara, R. Ishida, and M. Kasai.** 1998. RP58 associates with condensed chromatin and mediates a sequence-specific transcriptional repression. J. Biol. Chem. **273:** 26698–26704.
7. **Avitahl, N., S. Winandy, C. Friedrich, B. Jones, Y. Ge, and K. Georgeopoulos.** 1999. Ikaros set thresholds for T cell activation and regulates chromosome propagation. Immunity **10:**333–343.
8. **Bardwell, V. J., and R. Treisman.** 1994. The POZ domain: a conserved protein-protein interaction motif. Genes Dev. **8:**1664–1677.
9. **Besse, S., and F. Puvion-Dutilleul.** 1994. High resolution localization of replicating viral genome in adenovirus-infected HeLa cells. Eur. J. Cell Biol. **63:**269–279.
10. **Brown, K. E., J. Baxter, D. Graf, M. Merkenschlager, and A. G. Fisher.** 1999.

Dynamic repositioning of genes in the nucleus of lymphocytes preparing for cell division. Mol. Cell **3:**207–217.
11. **Cattoretti, G., C. C. Chang, C. Cechova, J. Zhang, B. H. Ye, B. Falini, D. C. Louie, K. Offit, R. S. K. Chaganti, and R. Dalla-Favera.** 1995. BCL-6 protein is expressed in germinal-center B cells. Blood **86:**45–53.
12. **Cook, P. R.** 1991. The nucleoskeleton and the topology of replication. Cell **66:**627–635.
13. **de la Luna, S., K. E. Allen, S. L. Mason, and N. B. La Thangue.** 1998. Integration of a growth-suppressing BTB/POZ domain protein with the DP component of the E2F transcription factor. EMBO J. **18:**212–228.
14. **Deltour, S., C. Guerardel, and D. Leprince.** 1999. Recruitment of the SMRT/N-coR-mSIN3A-HDAC repressing complex is not a general mechanism for BTB/POZ transcriptional repressors: the case of HI1 and gamma-FBP. Proc. Natl. Acad. Sci. USA **96:**14831–14836.
15. **Dent, A. L., A. L. Shaffer, Y. Xin, D. Allman, and L. Staudt.** 1997. Control of inflammation, cytokine expression and germinal center formation by BCL6. Science **276:**589–592.
16. **Depamphillis, M. L.** 1999. Replication origin in metazoans: facts or fiction? Bioassays **21:**5–11.
17. **Dhordain, P., O. Albagli, S. Ansieau, M. H. Koken, C. Deweindt, S. Quief, D. Lantoine, A. Leutz, J. P. Kerckaert, and D. Leprince.** 1995. The BTB/POZ domain targets the LAZ3/BCL6 oncoprotein and mediates homomerisation in vivo. Oncogene **21:**2689–2697.
18. **Dhordain, P., R. J. Lin, S. Quief, J. P. Kerckaert, R. M. Evans, and O. Albagli.** 1998. The LAZ3/BCL6 oncoprotein recruits a SMRT/SIN3/histone deacetylase-containing complex to mediate repression. Nucleic Acids Res. **26:**4645–4651.
19. **Dimitrova, D. S., and D. M. Gilbert.** 1999. The spatial positioning and replication timing of chromosomal domains are both established in early G1 phase. Mol. Cell **4:**983–993.
20. **Dunaway, M., J. Y. Hwang, M. Xiong, and H. L. Yuen.** 1997. The activity of the SCS and scs' insulator elements is not dependent on chromosomal context. Mol. Cell. Biol. **17:**182–189.
21. **Fuks, F., W. A. Burgers, A. Brehm, L. Hughes-Davies, and T. Kouzarides.** 2000. DNA methyltransferase dnmt1 associates with histone deacetylase activity. Nat. Genet. **24:**88–91.
22. **Gerasimova, T. I., and V. G. Corces.** 1995. Polycomb and Trithorax group proteins mediate the function of a chromatin insulator. Cell **92:**511–521.
23. **Guidez, F., S. Ivins, J. Zhu, M. Söderström, S. Waxman, and A. Zelent.** 1998. Reduced retinoic acid-sensitivities of nuclear receptor corepressor binding to PML- and PLZF-RARα underlie molecular pathogenesis and treatment of acute promyelocytic leukemia. Blood **91:**2634–2640.
24. **Hahm, K., B. S. Cobb, A. S. McCarthy, K. E. Brown, C. A. Klug, R. Lee, K. Akashi, I. L. Weissman, A. G. Fisher, and S. T. Smale.** 1998. Helios, a T-cell restricted Ikaros family member that quantitatively associates with Ikaros at centromeric heterochromatin. Genes Dev. **12:**782–796.
25. **Henderson, D. S., S. S. Banga, T. A. Grigliatti, and J. B. Boyd.** 1994. Mutagen sensitivity and suppression of position effect variegation result from mutations in *mus209*, the Drosophila gene encoding PCNA. EMBO J. **13:**1450–1459.
26. **Hozak, P., A. Bassim Hassan, and D. A. Jackson.** 1993. Visualisation of replication factories attached to a nucleoskeleton. Cell **73:**361–373.
27. **Hu, Y.-F., Z. L. Hao, and R. Li.** 1999. Chromatin remodeling and activation of chromosomal DNA replication by an acidic transcriptional activation domain from BRCA1. Genes Dev. **13:**637–642.
28. **Huang, E. Y., J. Zhang, E. A. Miska, M. G. Guenther, T. Kouzarides, and M. A. Lazar.** 2000. Nuclear receptor corepressors partner with class II histone deacetylases in a Sin3-independent repression pathway. Genes Dev. **14:**45–54.
29. **Huyhn, K. D., and V. Bardwell.** 1998. The BCL6 POZ domain and other POZ domains interact with the SMRT and NcoR corepressors. Oncogene **17:**2473–2484.
30. **Jackson, D. A., and A. Pombo.** 1998. Replicons clusters are stable units of chromosome structure: evidence that nuclear organization contributes to efficient activation and propagation of S phase in human cells. J. Cell Biol. **140:**1285–1295.
31. **Kao, H. Y., M. Downes, P. Ordentlich, and R. M. Evans.** 2000. Isolation of a novel histone deacetylase reveals that class I and class II deacetylases promote SMRT-mediated repression. Genes Dev. **14:**55–66.
32. **Katsani, K. R., M. A. Hajibagheri, and C. P. Verrijzer.** 1999. Co-operative DNA binding by GAGA transcription factor requires the conserved BTB/POZ domain and reorganizes promoter topology. EMBO J. **18:**698–708.
33. **Kerckaert, J. P., C. Deweindt, H. Tilly, S. Quief, G. Lecocq, and C. Bastard.** 1993. LAZ3, a novel zinc finger encoding gene is disrupted by recurring chromosome 3q27 translocations in human lymphomas. Nat. Genet. **5:**66–70.
34. **Kim, T. A., J. Lim, S. Ota, S. Raja, R. Rogers, B. Rivnay, H. Avraham, and S. Avraham.** 1998. NRP/B, a novel nuclear matrix protein, associates with $p110^{RB}$ and is resolved in neuronal differentiation. J. Cell Biol. **141:**553–566.
35. **Kim, J., S. Sif, B. Jones, A. Jackson, J. Koipally, E. Heller, S. Winandy, A. Viel, A. Sawyer, T. Ikeda, R. Kingston, and K. Georgeopoulos.** 1999. Ikaros DNA-binding proteins directs formation of chromatin remodeling complexes in lymphocytes. Immunity **10:**345–355.
36. **Koipally, J., A. Renold, J. Kim, and K. Georgeopoulos.** 1999. Repression by Ikaros and Aiolos is mediated through histone deacetylase complexes. EMBO J. **18:**3090–3100.
37. **Krude, T.** 1999. Mimosine arrests human cell proliferation before the onset of the DNA replication in a dose dependent manner. Exp. Cell Res. **247:**147–159.
38. **Krude, T., M. Jackman, J. Pines, and R. Laskey.** 1997. Cyclin-cdk dependent initiation of replication in a human cell-free system. Cell **88:**108–119.
39. **Kumagai, T., T. Miki, M. Kikuchi, T. Fukuda, N. Miyasaka, R. Kamiyama, and S. Hirosawa.** 1999. The proto-oncogene Bcl6 inhibits apoptotic cell death in differentiation-induced mouse myogenic cells. Oncogene **18:**467–475.
40. **Ma, H., J. Samarabandu, R. S. Devdhar, R. Acharya, P. C. Cheng, C. Meng, and R. Berezney.** 1998. Spatial and temporal dynamics of DNA replication sites in mammalian cells. J. Cell Biol. **143:**1415–1425.
41. **Ma, H., A. J. Siegel, and R. Berezney.** 1999. Association of chromosome territories with the nuclear matrix. Disruption of human chromosome territories correlates with the release of a subset of nuclear matrix proteins. J. Cell Biol. **146:**531–542.
42. **Nakayazu, H., and R. Berezney.** 1989. Mapping replicational sites in the eucaryotic nucleus. J. Cell Biol. **108:**1–11.
43. **Ohtsuki, S., and M. Levine.** 1998. GAGA mediates the enhancer blocking activity of the eve promoter in the Drosophila embryo. Genes Dev. **12:**3325–3330.
44. **Platero, J. S., A. K. Csink, A. Quintanilla, and S. Henikoff.** 1998. Changes in chromosomal localization of heterochromatin-binding proteins during the cell cycle in Drosophila. J. Cell Biol. **140:**1297–1306.
45. **Raff, J. W., R. Kellum, and B. Alberts.** 1994. The *Drosophila* GAGA transcription factor is associated with specific regions of heterochromatin throughout the cell cycle. Mol. Cell. Biol. **13:**5977–5983.
46. **Robinson, D. N., and L. Cooley.** 1997. Drosophila kelch is an oligomeric ring canal actin organizer. J. Cell Biol. **138:**799–810.
47. **Roth, S. Y., and C. D. Allis.** 1996. Histone acetylation and chromatin assembly: a single escort, multiple dances? Cell **87:**5–8.
48. **Sadoni, N., S. Langer, C. Fauth, B. Giogio, T. Cremer, B. M. Turner, and D. Zink.** 1999. Nuclear organization of mammalian genomes: polar chromosome territories build up functionally distinct higher order compartments. J. Cell Biol. **146:**1211–1226.
49. **Shibahara, K. I., and B. Stillman.** 1999. Replication-dependent marking of DNA by PCNA facilitates CAF-1 coupled inheritance of chromatin. Cell **96:**575–585.
50. **Smith, H. C., E. Puvion, L. A. Buchholtz, and R. Berezney.** 1984. Spatial distribution of DNA loop attachment and replicational sites in the nuclear matrix. J. Cell Biol. **99:**1794–1802.
51. **Sparvoli, E., M. Levi, and E. Rossi.** 1994. Replication clusters may form structurally stable complexes of chromatin and chromosomes. J Cell Sci. **107:**3097–3103.
52. **Wei, X., J. Samaradandu, R. S. Devdhar, A. J. Siegel, R. Acharya, and R. Berezney.** Segregation of transcription and replication sites into higher order domains 1998. Science **281:**1502–1506.
53. **Yarden, R. I., and L. C. Brody.** 1999. BRCA1 interacts with components of the histone deacetylase complex. Proc. Natl. Acad. Sci. USA **96:**4983–4988.
54. **Ye, B. H., G. Cattoretti, Q. Shen, J. Zhang, N. Hawe, R. D. Waard, C. Leung, M. Nouri-Shirazi, A. Orazi, R. S. K. Chaganti, P. Rothman, A. M. Stall, P. P. Pandolfi, and R. Dalla-Favera.** 1997. The BCL6 proto-oncogene controls germinal center formation and Th2-type inflammation. Nat. Genetics **16:**161–170.
55. **Ye, B. H., F. Lista, C. F. Lo, D. M. Knowles, K. Offfit, R. S. K. Chaganti, and R. Dalla-Favera.** 1993. Alterations of a zinc finger encoding gene, BCL6, in diffuse large cell lymphoma. Science **262:**747–750.
56. **Yoshida, C., F. Tokumasu, K. I. Hohmura, J. Bungert, N. Hayashi, T. Nagasawa, J. D. Engel, M. Yamamoto, K. Takeyasu, and K. Igarashi.** 1999. Long range interaction of cis-DNA elements mediated by architectural transcription factor bach1. Genes Cells **4:**643–655.